Simulation of coupled heat, air and moisture transfers in an experimental house exposed to natural climate

Matthieu Labat, Monika Woloszyn, Géraldine Garnier, Amanduine Piot, Jean-Jacques Roux

Building Simulation 2013, 13th International conference of the International building performance simulation association
Chambéry, France, August 26-28

SIMULATION OF COUPLED HEAT, AIR AND MOISTURE TRANSFERS IN AN EXPERIMENTAL HOUSE EXPOSED TO NATURAL CLIMATE

Matthieu Labat[1,2], Monika Woloszyn[3], Géraldine Garnier[2], Amandine Piot[2,4] and Jean-Jacques Roux[1]
[1]CETHIL, Université de Lyon, CNRS, INSA-Lyon, CETHIL, UMR5008, F-69621, Villeurbanne, France
[2]CSTB - 24 rue Joseph Fourier, 38400 Saint Martin d'Hères, France
[3]Laboratoire Optimisation de la Conception et Ingénierie de l'Environnement (LOCIE), CNRS-UMR5271, Université de Savoie, Campus Scientifique, Savoie Technolac, 73376 Le Bourget-du-Lac Cedex, France
[4]CEA, 50 avenue du Lac Léman | F-73375 Le Bourget-du-Lac, France

ABSTRACT

Detailed experimental studies of heat and moisture transfers in building envelope parts are important to gain knowledge about hygrothermal responses and to validate models. For this purpose, a 20 m^2 wooden-frame test house built in Grenoble, France, was widely instrumented to collect temperature and relative humidity at different depths in the wall, as well as indoor and outdoor conditions. Besides, a general simulation tool was selected to simulate coupled transfer at the building scale.

In this paper, an experimental sequence is presented and simulated. Simulation results met temperature and humidity measurements within the walls, which give confidence in the model relevancy. Therefore, moisture and heat balances were applied at the building scale.

INTRODUCTION

Constructing buildings that achieve energy efficiency is an ongoing research topic which has overtaken the study of heat transfer only. For example, it is relevant to study the coupling of heat, air and moisture transfers in the building envelope. A whole international study named "Annex 41" was dedicated to this subject which and organized by the IEA (International Energy Agency). In this work, several simulation tools were compared to a simple test case and notable differences were observed. This underlined the need of more experimental results to validate the numerical models.

Many experiments have been achieved for various scale and boundary conditions. Recently, (Belleghem *et al.* 11) presented a state of art of experimental work on moisture transfers in porous media. Then, the authors have studied moisture transfers between a 0.04 m^2 sample and indoor air. At the wall scale, (Vinha 07) presents measurements achieved on different wall types for various controlled conditions. Another experience at the wall scale is reported in (Desta *et al.* 11), but one siding is exposed to real outdoor conditions. At the building scale, fewer experiments can be found in literature. Moreover, most focus on specific transfers. For example, (Simonson 05) measured the energy consumption of an inhabited house in Finland. (Langmans *et al.* 10) measured the air permeability in Belgian dwellings and discussed about the influence of vapor barriers.

Therefore, there is a lack of experimental data concerning coupled transfers at the building scale exposed to real climate conditions.

For this purpose, a 20 m² wooden frame test-house was built in Grenoble, France. The set-up was widely instrumented to collect temperature and relative humidity at different depths in the wall, as well as indoor and outdoor conditions. Coupled transfers were simulated with HAM-Tool libraries, which are based on Simulink / Matlab software (Kalagasidis *et al.* 07). It has been successfully validated through a numerical comparison with other models as presented in (Woloszyn and Rode 08).

At the building scale and under natural exposure, many transfers are occurring simultaneously, hardening the identification of the most sensitive transfers, and somehow, the validation of simulation tools. For this reason, earliest studies were dedicated to the validation of specific coupled transfers:

- Coupled heat and vapour transfer in the insulated part of vertical walls.
- Bi-dimensional effects induced by the ventilated cavity (Labat et al. 2012a).
- Air change rate occurring under natural conditions (Labat et al. 2012b).

Based on these results, this paper aims at proposing a simulation of coupled heat, air and moisture transfer at the building scale. Computed results will be set against measurements achieved during a 15 days long experiment and general conclusions will be drawn.

The first part of this paper gives an overlook on the experimental set-up. The measured indoor and outdoor conditions recorded during the experience will also be presented. The second part deals with modelling considerations. In the last part, simulation results will be set against measurements and discussed.

EXPERIMENTAL CONSIDERATIONS

Description of the experimental set-up

The experimental house is located close to Grenoble, France (latitude: 45.2°E, longitude: 5.77°N) and is exposed to natural climate (see Fig. 1). It is divided into one main room and a naturally ventilated attic. The dimensions of the main room were designed to be representative for a living room (4.56×4.55×2.36 m^3 interior dimensions, so its volume is

approximately 49 m^3). The roof is a typical tiled French roof with two 30° slopes facing north and south. The door, which is the only opening into the test house, is located in the middle of the northern side.

Fig. 1: Picture of the experimental set up (western and northern sides) with location of the ventilation opening

To ease the study of coupled transfers, this set-up was designed to minimise the transfers through horizontal walls. To do so, the floor was elevated 0.57 m above the ground and the insulation of both the ceiling and the floor was increased (4×100 mm of mineral wool, two layers of vapour barrier which are equivalent in terms of vapour diffusion to a 150 m thick air layer). On the indoor side, the ceiling was covered with gypsum board (13 mm), and the floor with OSB panels (18 mm).

The door of the test house, located in the middle of the northern face, was insulated with polystyrene so the insulation level is homogeneous on the whole face.

The structure of the vertical walls is made of spruce studs (section: 0.07×0.165 m^2), positioned every 0.60 m. The insulated part of the wall, which is of main interest here, is presented in Fig. 2 and is composed of the following elements:

- a gypsum board on the indoor side (0.013 m)
- a vapour barrier made out of polyethylene (equivalent to a 18 m thick air layer)
- cellulose wadding used as an insulation material between the spruce studs (0.160 m)
- a particle board on the outdoor side (0.100 m)
- a rain screen made out of polypropylene
- a 0.027 m wide ventilated air gap
- a wooden cladding (0.020 m)

The cladding is open-jointed: it is made up of boards with typical dimensions 5×0.08×0.02 m (L×H×l) which are vertically spaced to create a 0.008 m high air gap between two adjacent boards. As the gaps are small (less than 10% of the surface) and slanted, they are not visible on the general photography presented in Fig. 1. Vertical cleats located behind the cladding make it possible to maintain six boards in a row. The vertical cleats are spaced every 0.60m and are continuous from the bottom to the top of the cladding, dividing the air gap into independent regular cavities of 0.60×0.027×3.80 m^3.

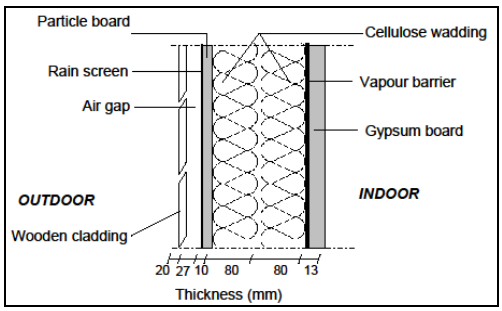

Fig. 2: Scheme of a vertical wall section

The test house is also equipped with a ventilation system that is located in the attic: the indoor opening is located in the ceiling while the outdoor opening is located close to the eaves on the western face, 3.43 m up the wall of the experimental house, as shown in Fig. 1. Further details about the test house can be found in Piot *et al.* (2011).

Material properties

Thermal properties of dry materials have been measured in laboratory at 23°C. The results are presented in Table 1.

Table 1: Thermal properties on dry materials

Material	ρ_{Dry} ($kg.m^{-3}$)	λ_{Dry} ($mW.m^{-1}.K^{-1}$)	Cp_{Dry} ($J.kg^{-1}.K^{-1}$)
Plaster board	712.5	190	1010
Cellulose wadding	50	42	1100
Particle board	700.2	106.7	1270
Spruce	366.9	90.1	1300
OSB	602	95.3	1450

Table 2: Humid thermal conductivity and vapour permeability

Material	λ_W $W.m^{-1}.K^{-1}$ $.(kg.m^{-3})^{-1}$	δ-dry cup 10^{-12} s	δ-wet cup 10^{-12} s
Plaster board	$1.67.10^{-3}$	21.7	29.8
Cellulose wadding	N/A (1)	7.79	17.4
Particle board	$1.28.10^{-4}$	2.11	2.79
Spruce	$5.1.10^{-4}$	1.08 (2)	25 (2)
OSB	$2.0.10^{-4}$	1.81	1.88

(1) No change observed in thermal conductivity for RH varying from 0 to 90 %
(2) Values coming from Kumaran *et al.* 2002

As there is also interest in vapour transfers, the humid thermal conductivity, the vapour permeability and the sorption isotherm have been measured. The humid thermal conductivity is defined as follow:

$$\lambda(w) = \lambda_{Dry} + \lambda_W \cdot w \quad (1)$$

The vapour permeability was measured with the cup method (dry and wet cup), according to the standard NF EN ISO 12572. The samples were placed between environments at 0 and 50 % RH for the dry cup, 50 and 94 % RH for the wet cup. Results are presented in Table 2.

The sorption isotherm (23°C) was measured according to the standard NF EN ISO 12571. The moisture content equilibrium values are presented in Fig. 3. It is the average values obtained with three samples and correspond to the first adsorption curve. No measurements were made for desorption or above 95 % RH.

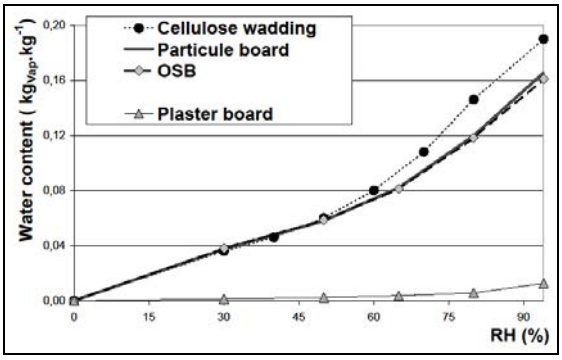

Fig. 3: Comparison of the sorption isotherms of the different materials

Monitoring temperature and humidity inside the walls

Fig. 4 shows the positions of the sensors located in the eastern and western walls, at mid-height and at different depths within the walls. Thermo-hygrometers (HRT 2 and HRT 3) allow measuring directly the impact of the vapour barrier on vapour transfer.

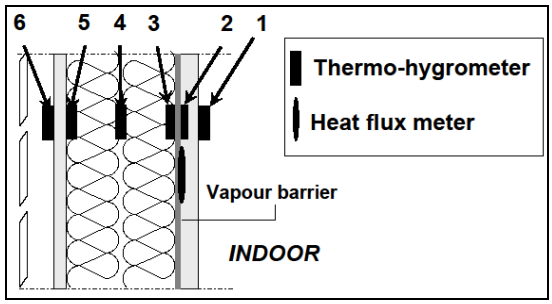

Fig. 4: Positions of the sensors in the vertical walls

Concerning both the northern and southern walls, only 2 thermo-hygrometers were installed (corresponding to HRT 2 and HRT 4). Additional sensors were installed at various locations within the walls, mostly thermocouples in the eastern wall. They will not be discussed in this paper, but more details can be found in (Piot *et al.* 11). The number and accuracy of the sensors used with this set-up are presented in Table 3.

Table 3: Number and accuracy of the sensors

Type	Number	Accuracy
Thermo-hygrometer	55	±5 % RH ±0.8°C
Pt100	1	±0.03°C at 0°C
Heat flux meter	7	± 3 %
T-type thermocouple	87	± 1°C

Outdoor conditions

This paper presents a specific experiment which took place from 01/02/2012 to 14/02/2012. Local weather conditions were determined with an on-site station which recorded the climatic conditions every 10 min. As it can be seen in Fig. 5, outdoor temperature remained negative during this experiment.

When focusing on vapour transfer, it is convenient to consider relative humidity as it can be easily measured. Still, its study can be tricky as it depends strongly on temperature. Therefore, many authors prefer to consider vapour pressure, which is the potential governing vapour transfer (Carmeliet and Derome 12, Piot *et al.* 11). Absolute humidity (AH) represents the mass ratio of water in dry air and is derived from vapour pressure as shown in (2). It was selected here to study vapour transfer as it is directly representing mass balance equation.

$$AH = \frac{r_{Vap}}{r_{DA}} \cdot \frac{p_{Vap}(HR,T)}{p_{Tot} - p_{Vap}(HR,T)} \quad (2)$$

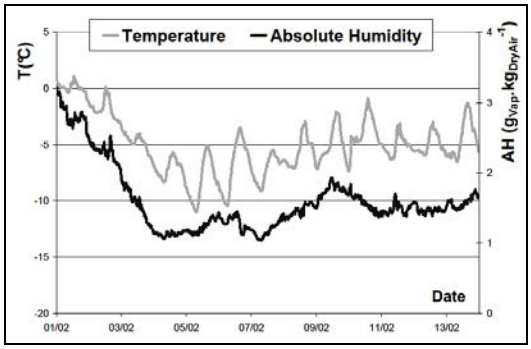

Fig. 5: Outdoor temperature and absolute humidity measurements

Based on direct and diffuse solar irradiance measurements, direct irradiance on vertical walls was computed and results are plotted in Fig. 6 for different orientation. It overreached 600 W.m^{-2} on eastern and southern sides several days.

Finally, wind speed and direction were measured 8 m above the ground. The corresponding wind rose is

presented in Fig. 7 and mean wind velocity was 3.8 $m.s^{-1}$.

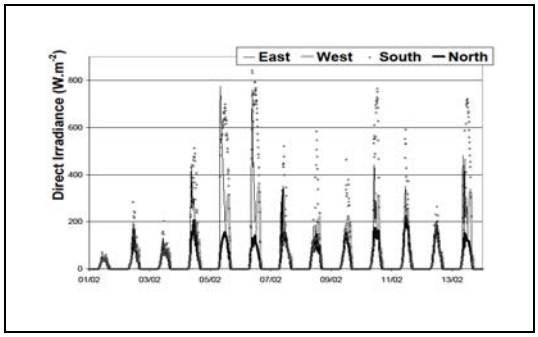

Fig. 6: Direct irradiance for each orientation

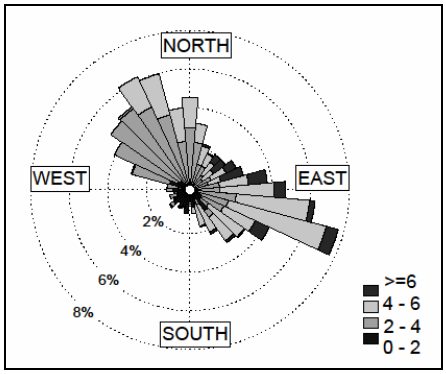

Fig. 7: Measured wind rose

Indoor conditions

The indoor temperature and relative humidity were measured by the mean of six thermo-hygrometers located at different heights and a Pt100 sensor. In order to have homogeneous indoor conditions, a fan mixes indoor air. During this experiment, a simple scenario was simulated by the mean of a convective heater and a vapour generation system (cold mist generator).

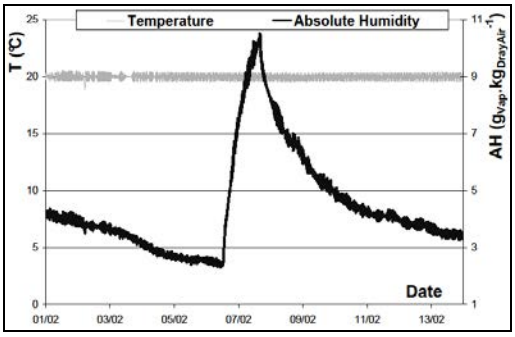

Fig. 8: Indoor temperature and absolute humidity measurements

For three months preceding the experiment and during the period of interest here, indoor temperature was maintained at 20 ±1 °C. Vapour was generated during approximately 28 hours, from 06/02/2012 to 07/02/2012. The exact production rate was measured by weighing the generator. It appeared to be constant (around 200 $g.h^{-1}$), so the total amount of generated vapour reached almost 6 kg. This resulted in an increase of the indoor absolute humidity from 2.5 to 10.5 $g_{Vap}.kg_{DryAir}^{-1}$ as shown in Fig. 8.

Finally, the ventilation system remained turned off during the whole experiment, yet air was free to move across the ventilation opening.

SIMULATION CONSIDERATIONS

Simulating transfers in the insulated part of walls

HAM-Tools library was used directly to model one dimensional coupled transfer in the insulated part of walls, assuming the following simplifications were still valid:

- There was no airflow crossing the insulated part of the wall;
- Moisture content remained low enough to assume the super-hygroscopic state was never reached. Therefore, vapour transfer was governed by vapour pressure only and liquid transport was not acting;
- The enthalpy of moisture content in the materials and the latent heat effect were included in energy balance ;
- Measured material properties were taken into account and were updated according to actual moisture content at every time step for each node.

The walls were meshed with nineteen nodes: ten for each siding and nine for the insulating material as illustrated in Fig. 9. In order to allow precise comparison with measurements, the nodes set close to the sensors locations were sized down to 0.5 mm in the sidings, 1.5 mm in the insulating material. The solution was validated to be independent from chosen mesh by comparing results obtained with other meshes.

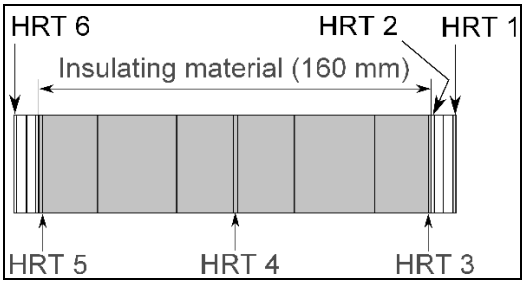

Fig. 9: Mesh applied to the insulated part of the vertical wall for the one-dimensional simulations and sensors location

Simulation results were found to be in good agreement with measurements in most cases, that is to say within the uncertainty range. However, the model failed to predict absolute humidity variations under specifically complex conditions; precisely, higher differences occurred when a vapour flux coming from indoor was meeting a reversed vapour transfer. This latest phenomena may occur under

high temperature variations on the outdoor sidings, and is known as a sun-driven vapour transfer (Carmeliet and Derome 12, Piot *et al.* 11). Still, this resulted not in a significant bias on the long term.

Simulating transfers in the ventilated cavity

In an earlier study (Labat *et al.* 2012a), a strong bi-dimensional effect induced by the wooden cladding and the air gap was shown. To include this phenomenon, the above mentioned wall model was enhanced to include the modelling of coupled heat and air transfer in the ventilated cavity.

The general pattern is presented in Fig. 10 and consists in dividing in seven parts each single vertical wall. Coupled transfers were still modelled on a one-dimensional point of view in solid parts. In the ventilated cavity however, the vertical effect was modelled.

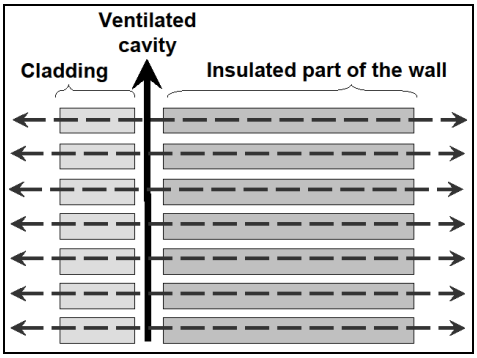

Fig. 10: Modelling scheme of the bi-dimensional effect induced by the ventilated cavity

Air transfer was relying on a semi-empirical correlation presented in (Labat *et al.* 2012a) while heat transfer was described using general literature results. Results were set against measurements achieved under rough summer conditions for both eastern and western walls. Computed heat fluxes were integrated on 24 hours basis and found to be 8 % accurate.

Simulating air transfers at the building scale

A classical single-node pressure model was previously selected to estimate the global air change rate (Labat *et al.* 2012b). General correlations were used to represent both wind and thermal effects. Experimental measurements, based on air permeability and the tracer gas techniques, were used to fit numerically obtained wind and thermal coefficient values. The computed global air change rate was estimated to be 23 % accurate. It was also shown that the model represented the best measurements for average outdoor conditions, while higher differences occurred under wind speed higher than 3 $m.s^{-1}$.

Building simulation and general inputs

The outdoor conditions presented in the previous section were used as boundary conditions so a simulation of coupled transfer acting at the building scale could be achieved. It included the modelling of the vertical walls and the ventilated cavities, the indoor volume and the air change rate. Transfers across the floor, the ceiling, the door and the structure were not simulated because they were still not validated. However, vapour transfer in all indoor sidings, including the horizontal surfaces and the door, were taken into account.

Vapour production was simulated according to mass measurement and heat production was set so the measured indoor temperature could was attained. Indoor air volume was modelled as a single node. Its temperature and humidity were not fixed but resulted from transfers with indoor sidings, the production of heat and vapour and from the impact of the air change rate. Somehow, it indicates how accurate the model is at the building scale.

Constant values were used for convective heat and mass transfer coefficients ($h_{C,In}$, $h_{Vap,In}$ and $h_{Vap,Out}$) and indoor irradiative coefficient ($h_{Irr,In}$). A three-month experiment under stable indoor conditions was used to fit these values (not presented here). The results are presented below:

- $h_{C,In} = 6\ W.m^{-2}.K^{-1}$;
- $h_{Irr,In} = 4\ W.m^{-2}.K^{-1}$;
- $h_{Vap,In} = 1.10^{-8}\ s.m^{-1}$;
- $h_{Vap,Out} = 1.10^{-8}\ s.m^{-1}$.

Initial conditions were set using temperature and relative humidity measurements recorded on 01/02/2012 00h00 for the nodes set at sensor locations and interpolated for the others.

RESULTS AND DISCUSSION

For the sake of clarity, only few significant results will be presented and discussed in this section. Therefore, it was decided to show results where the highest differences were observed, here in the southern oriented wall. First, the discussion will focus on local temperatures and absolute humidity levels. Once validated, this will allow considering heat and moisture transfer on a larger scale.

Temperature inside the southern vertical wall

Temperature measurements are plotted against simulation results at three different depths in Fig. 11 (see Fig. 4 for the sensor locations).

On both sides of the indoor siding (HRT 1 and HRT 3), the difference between measurements and simulation results is lower than the measurement uncertainty (± 0.8 °C). Between the insulating material and the outdoor siding however (HRT 4), higher differences occurred. Precisely, they overreached 3°C four times. For other wall orientations however, such high difference was never observed.

This is probably a direct consequence of the ventilated cavity modelling. It relies on

measurements achieved on the eastern and western sides, which geometries are identical. On the other hand, the southern ventilated cavity geometry is noticeably different (it is smaller and the roof overhang is much longer), therefore the ventilated cavity behaviour may differ significantly.

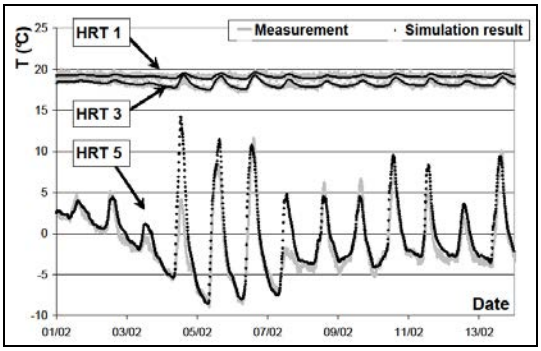

Fig. 11: Temperature measurements in the southern wall (full lines) and simulation results (black dots)

Nevertheless, temperature differences were occasional and did not affect much the global energy behaviour. This can be seen in Fig. 12, where heat flux measurements were integrated over 24 hours and found to meet simulation results within 3 %.

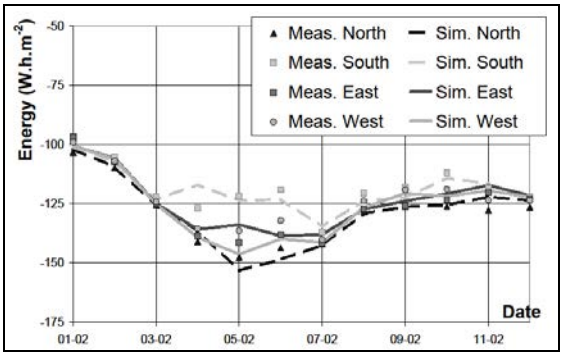

Fig. 12: Comparison of heat flux measurement integrated over a whole day with simulation results for each orientation

Heat balance applied to the building scale

The current model is able to represent correctly the general thermal behaviour of the vertical walls. To give an idea on its applicability, one could compute a heat balance applied to the building scale. Here, six heat fluxes were distinguished: the heat source $\Phi_{Heating}$, heat transfer through vertical walls $\Phi_{Vertical\_Walls}$, through horizontal walls $\Phi_{Floor+Ceiling}$ and through the spruce structure and the door $\Phi_{Structure}$, the impact of the air change rate Φ_{ACH}, and a last term which includes three-dimensional effects Φ_{3D} (the so-called thermal bridges). This sixth term can be deduced from the heat balance as presented in (3).

$$-\phi_{3D} = \phi_{Heating} + \phi_{Vertical\_Walls} + \phi_{Floor+Ceiling} + \phi_{Structure} + \phi_{ACH} \quad (3)$$

Three terms included in the heat balance were not studied in detail, yet they can be quickly estimated. As first order, thermal resistances of the floor, the ceiling, the structure and of the door were calculated based on the measured dry thermal conductivity (see Table 1) and thicknesses. Results are presented in Table 4. Then heat fluxes were computed using measured boundary temperatures.

Table 4: Estimated thermal resistance for unstudied building parts

	Floor + Ceiling	**Spruce structure**	**Door**
R_{Th} ($m^2.K.W^{-1}$)	13.0	2.0	4.5
S (m^2)	41.4	5.9	1.8

Heat fluxes were integrated on 24 hours, similarly to Fig. 12. Results are presented in Fig. 13, where energy losses are plotted negatively.

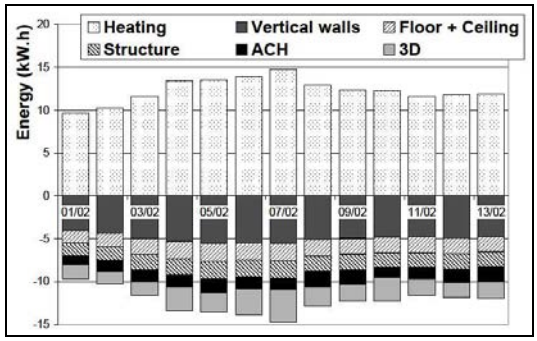

Fig. 13: Heat balance applied to indoor air

A day-averaged 12 kWh energy consumption was measured over this whole experiment. The sharing of the losses was not significantly varying from one day to another and the average values are presented in Table 5.

Table 5: Estimated sharing of the energy losses

	Vertical Walls	**Floor + Ceiling**	**Structure + Door**	**ACH**	**3D**
Share	41 %	15 %	14 %	12 %	18%

It came out the heat transfers analysed in detailed in the present work, namely "vertical walls" and "ACH", are equivalent to half of the total energy losses. However, other transfers are not completely unknown. For example, the floor, and ceiling could be modelled similarly to vertical walls, however the outdoor boundary conditions should be carefully defined. Indeed the ceiling is in contact with unheated ventilated attic, and the floor with an open air space under the experimental facility (see Fig 1). Modelling wood-based components such as the structure and the door would require much detailed work; the coupling between heat and vapour transfer is bound to be more complex, the one-dimensional assumption could not apply and material properties should be defined much in detail.

Moisture inside the southern vertical wall

Absolute humidity measurements are plotted against simulation results in Fig. 14, for the same positions as used for temperature measurements in Fig. 11.

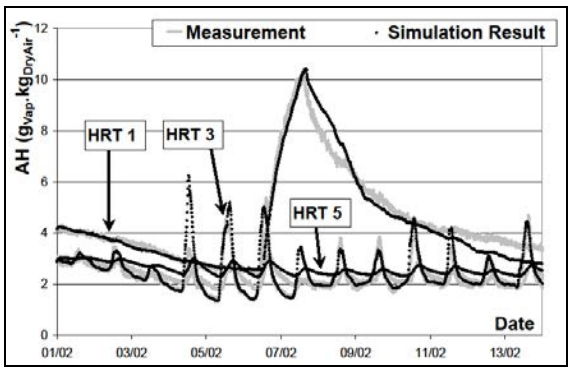

Fig. 14: Absolute humidity measurements in the southern wall and simulation results (black dots)

First, the model behaves correctly indoor (HRT 1) during the whole experiment. This means vapour transfers at the building scale were correctly identified and described. Higher differences were observed at the end of the experiment. It probably came from the air change rate calculation, which accuracy is lowered under wind velocities higher than 3.0 $m.s^{-1}$ (the average velocity was 3.8 $m.s^{-1}$ during this experiment).

Second, vapour transfer in the insulating material was not influenced by indoor climate because of the vapour barrier. On the other hand, temperature variations on the outdoor siding were high enough to prompt vapour transfer (the "sun-driven vapour transfer", as presented in the previous section). As a consequence, differences in absolute humidity were the highest as soon as temperature was poorly estimated (04/02, 07/02).

Finally, a 0.4 $g_{Vap}.kg_{DryAir}^{-1}$ bias was observed at the end of the experiment, which is still within the uncertainty range. This may results from the rather rough determination of initial values. As boundary conditions were varying, vapour transfer was occurring previously to the start of the main experiment. This might lead to non-uniform moisture profile within materials, particularly for those with a high sorption capacity. However, such a profile is hard to describe using available measurements. To limit the influence of the selected initial values, one should start the simulation one month at least before the considered experiment. Unfortunately, this was unfeasible in this case because of the accidental loss of the weather data.

Moisture balance applied to indoor air

Even if some differences were observed, the average measured humidity levels were correctly estimated at different depths in the walls. More, the indoor level was in good agreement with measurements, which is noticeable. Therefore, it is possible to propose a moisture balance applied to the indoor air volume as presented in (4). Here, four terms were identified: vapour production $G_{Generator}$, the impact of the air change rate G_{ACH}, vapour transfer with the indoor sidings G_{Walls} and the storage capacity of the indoor air itself G_{Indoor}.

$$G_{Generator} + G_{ACH} + G_{Walls} + G_{Indoor} = 0 \quad (4)$$

Vapour fluxes were integrated over 24 hours and results are plotted in Fig. 15. Positive fluxes are representing the indoor air gaining water vapour (from the generator for example).

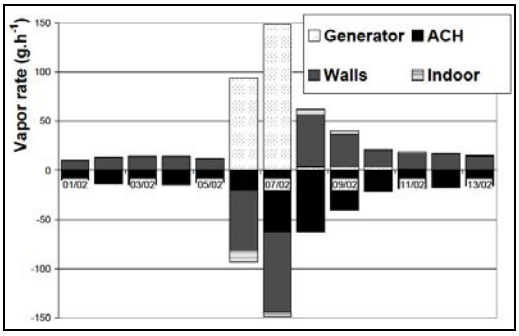

Fig. 15: Moisture balance applied to indoor air

Before the vapour generator was turned on (from 01/02 to 05/02), the air renewal was drying out indoor air because of the very low absolute humidity level outdoor (< 2.0 $g.kg_{DryAir}^{-1}$, see Fig. 5). However, indoor sidings partly softened this decrease.

During vapour production, 32 % of the vapour was evacuated by air infiltrations, 60 % was adsorbed by the sidings and only 8 % remained in the air volume. As soon as the generator was shut down, indoor humidity was decreasing because of the air renewal. Once again, the indoor sidings were slowing this decrease. This illustrates the hygroscopic buffering capacity of indoor material.

This model could be used to compare different envelope types and to predict the energy saving due to the replacement of some parts of the envelope.

CONCLUSION AND OUTLOOK

In this paper, an experimental wooden-frame house exposed to natural conditions was used to validate a building performance simulation tool. A 15 days long experiment was defined; it occurred under cold outdoor conditions while almost 6 kg of water vapour were released indoor during 2 days.

An existing model named HAM-Tools was selected to simulate coupled heat and moisture transfer in the insulated part of the vertical walls, the air change rate at the building scale, and vapour transfer with indoor sidings. Studies dedicated to these specifics parts were achieved earlier, making it easier to simulate transfer at the building scale.

Results were first discussed on a local point of view, with looking at temperature and absolute humidity measurement within the walls. As the model

represented correctly the global behaviour, it gave confidence to compute heat and vapour balance at the building scale.

Computed heat balance showed half the energy losses were taken into account by the current model in a great detail. To go on further, one should define the boundary conditions for the horizontal surfaces, validate coupled transfer taking place in the structure and take into account three dimensional transfers. On the other hand, all moisture fluxes impacting indoor conditions are well represented. Computed moisture balance illustrated the buffering capacity of indoor materials, and its effect on smoothing indoor humidity variations.

This model could be developed further to represent the whole coupled transfers which occur at the building scale. Also, it can be used to compare different wall assemblies and draw general conclusion on their energy and durability performances.

NOMENCLATURE

AH = *absolute humidity* ($kg_{Vap}.kg_{DryAir}^{-1}$)
Cp = *heat capacity* ($J.kg^{-1}.K^{-1}$)
G = *vapour flux* ($kg.s^{-1}$)
p_{Vap} = *vapour pressure (Pa)*
p_{Tot} = *total pressure (Pa)*
RH = *relative humidity (%)*
R_{Th} = *thermal resistance* ($m^2.K.W^{-1}$)
r_{DA} = *Dry Air constant = 287* $J.kg^{-1}.K^{-1}$
r_{Vap} = *Vapour constant = 462* $J.kg^{-1}.K^{-1}$
S = *surface* (m^2)
T = *temperature (°C)*
w = *water content* ($kg_{Vap}.m^{-3}$)

δ = *vapour permeability (s)*
λ = *thermal conductivity* ($W.m^{-1}.K^{-1}$)
λ_W = *humid thermal conductivity* ($W.K^{-1}.kg^{-1}.m^2$)
Φ = *heat flux (W)*

ACKNOWLEDGEMENT

This work has been supported by ADEME (the French Environment and Energy Management Agency, OPTI-MOB project, n°0704C0099) and by French Research National Agency (ANR) through "Habitat intelligent et solaire photovoltaïque Program" (project HYGRO-BAT n°ANR-10-HABISOL-005).

REFERENCES

Belleghem, M.V., Steeman, M., Willockx, A., Janssens, A., De Paepe, M., 2011. Benchmark experiments for moisture transfer modelling in air and porous materials. Building and Environment 46, p.884–898.

Carmeliet, J., Derome, D., 2012a. Temperature driven inward vapour diffusion under constant and cyclic loading in small-scale wall assemblies: Part 1 experimental investigation, Building and Environment 48, 48-56.

Desta, T.Z., Langmans, J., Roels, S., 2011. Experimental data set for validation of heat, air and moisture transport models of building envelopes, Building and Environment, 46 (5), p.1038-1046

Kalagasidis, A.S., Weitzmann, P., Nielsen, T.R., Peuhkuri, R., Hagentoft, C.E., Rode C., 2007. The international building physics toolbox in simulink, Energy and Building 39 (6) 665-674

Kumaran K., Lackey J., Normandin N., Tariku F., van Reenen, D., 2002. A thermal and moisture transport property database for common building and insulating materials, Final Report from ASHRAE Research Project 1018-RP.

Labat M., Woloszyn M., Garnier G., Rusaouen G., Roux J.J., 2012a. Impact of direct solar irradiance on heat transfers behind an open-jointed ventilated cladding: experimental and numerical investigations, Solar Energy 86, p.2549-2560

Labat M., Woloszyn M., Garnier G., Roux J.J., 2012b. Assessment of the air change rate of airtight buildings under natural conditions using the tracer gas technique. Comparison with numerical modelling, Building and Environment 60, p.37-44

Langmans, J., Klein, R., De Paepe, M., Roels, S., 2010. Potential of wind barriers to assure airtightness of wood-frame low energy constructions. Energy and Buildings 42, p.2376–2385.

Piot A, Woloszyn M, Brau J, Abele C., 2011. Experimental wooden frame house for the validation of whole building heat and moisture transfer numerical models, Energy and Buildings 43, p.1322-1328

Simonson, C., 2005. Energy consumption and ventilation performance of a naturally ventilated ecological house in a cold climate. Energy and buildings 37, p.23–35.

Vinha J., 2007. Hygrothermal performance of timber-framed external walls in Finnish climatic conditions: a method for determining the sufficient water vapour resistance of the interior lining of a wall assembly, Thesis, Tampere University of technology, Tampere, Finland.

Woloszyn, M., Rode, C., 2008. Tools for performance simulation of heat, air and moisture conditions of whole buildings, Building Simulation: an international journal 1, 5-24.